Modeling Tumour Growth with a Modulated Game of Life Cellular Automaton Under Global Coupling

Vladimir García-Morales, José A. Manzanares, and Javier Cervera

Abstract We propose a coupled map lattice that simulates the Gompertz tumour growth model used in cancer diagnosis and is able to reproduce the long-time parameter correlations that have been found in previous studies. The coupled map lattice is a modulated Game of Life cellular automaton model that includes only two free parameters. Parameter γ governs the strength of a global coupling of the cells due to the confinement pressure. Parameter κ governs the strength of the intercellular coupling which modulates the local dynamic rules of Conway's Game of Life.

1 Introduction

Tumours are self-organizing, complex systems, that must be studied and treated as such on a micro- and macroscopic level [1]. Macroscopically, a widely-used phenomenological model of tumour growth is Gompertz model, which describes the evolution of the tumour volume V as a function of time t as [2–7]

$$V(t) = V_0 \exp\left(\frac{A}{B}\left(1 - \exp(-Bt)\right)\right) \tag{1}$$

where V_0 is the volume at time $t = 0$, and A and B are parameters. At times $t \ll 1/B$, Eq. (1) reduces to $V = V_0 \exp(At)$ (exponential growth). At the later stages of tumour growth, $t \gg 1/B$, the volume attains a maximum value $V_{\max} := V_0 \exp(A/B)$. A remarkable empirical correlation found experimentally by Norton et al. [5] is that parameters A and B seem to be correlated as

$$\exp A = a \ln B + b \tag{2}$$

V. García-Morales (✉) · J. A. Manzanares · J. Cervera
Departament de Física de la Terra i Termodinàmica, Universitat de València,
46100 Burjassot, Spain
e-mail: vladimir.garcia@uv.es

I. Balaz and A. Adamatzky (eds.), *Cancer, Complexity, Computation*,
Emergence, Complexity and Computation 46,
https://doi.org/10.1007/978-3-031-04379-6_5

where a and b are constants that depend on the type of tumour. This correlation has the following important implication in cancer diagnosis: By determining the coefficient A from early stages of tumour development (in which the growth is exponential), parameter B dictating the characteristic time $\tau_c = 1/B$ that marks the transition between early and late stages of tumour development can be predicted from Eq. (2) as $B = \exp[(-b + \exp A)/a]$. Consequently, the maximum tumour volume $V_{\max}$ to be attained at later stages of growth can be predicted, as well as the whole function $V(t)$ in Eq. (1).

The Gompertz equation is useful for describing tumour growth, but it does not reflect any microscopic mechanisms [8]. This fact has motivated some researchers to devise cellular automata models to explain Gompertzian tumour growth as an emergent behavior. In a pioneering work, Qi et al. [8] considered a probabilistic cellular automaton with four different types of cells over a von Neumann neighborhood dependent on six parameters (three of which could be fixed by experiments, the remaining being free). One of the free parameters d_c was meant to account for the effect of the confinement mechanical pressure: a tumour can only expand if its inner pressure is larger than the external pressure, a fact that dynamically constrains the maximum tumour size. However, d_c was related to the distance of the cells to the origin, placed at the center of the lattice, therefore treating the center of the lattice in a different way to the rest of the lattice (the translational symmetry characteristic of any cellular automaton being broken). If we consider that a tumour can equally originate at any other region of the lattice, such symmetry breaking introduces, in our opinion, an undesirable feature since it not only limits the number of physically meaningful initial conditions (requiring cancerous cells to be necessarily at the center of the lattice for a tumour to grow): it also introduces a preferred reference frame that is unjustified. This feature is also present in the work by Kansal et al. [9] who presented a probabilistic 3D cellular automaton model depending on four free parameters on a Voronoi lattice, which is more dense at the center where the tumour was initially placed. The above mentioned works, [8, 9], discussed two different kinds of tumours actually found in biological systems. Qi et al. considered the most common type in which the tumour can be active not only at its surface but also in its interior, e.g., the mouse carcinoma KHT and the spontaneous carcinoma C3H in mice [8]. Kansal et al. considered activity of the tumour only at its surface, the interior of the tumour being composed of necrotic, inactive cells, as it is found in the glioblastoma multiforme in the brain [9]. Both models satisfactorily account for Gompertzian growth as described by Eq. (1). However, the empirical correlation shown in Eq. (2), which seems to be apparent in realistic tumour growth, was not addressed in Refs. [8, 9].

In this work, we present a 2D coupled-map lattice model based on cellular automata dynamics [10, 11] under global coupling. Our model has only two free parameters, predicts Gompertzian tumour growth given by Eq. (1) as well as the correlation between the parameters, Eq. (2), found in Ref. [5]. The local dynamical rules of the model are similar to those of Conway's Game of Life [12–16] but are modulated by a coupling parameter κ. The other free parameter γ accounts for the global confinement pressure and is called the strength of the global coupling.

2 Model

We represent a cell in the multicellular ensemble as a site in a 2D square lattice with $\Omega = n^2$ sites, where n is the number of sites on a side of the lattice. The dimensionless, continuous variable $u_t^{i,j}$ represents the dynamical state of the cell at site (i, j) at time t; hereinafter we refer to the state of the cell as the state of the site. We say that the site (i, j) is normal when $u_t^{i,j} \leq 0.15$ and that it is cancerous when $u_t^{i,j} > 0.15$. A lattice where most sites are found in state 0 is said to be normal, i.e. composed of normal non-cancerous cells. The total number of abnormal cells in the lattice is counted as

$$N_{ab} = \sum_{i=1}^{n} \sum_{j=1}^{n} H(u_t^{i,j} - 0.15) \tag{3}$$

where $H(x)$ is the Heaviside step function ($H(x) = 1$ if $x > 0$ and $H(x) = 0$ otherwise). The tumour volume is $V = N_{ab} v_0$, where v_0 is the "volume" of a single cell in the lattice.

The biological signals that couple individual cells to their local multicellular environment may contribute to normalization and are modeled using a continuous parameter κ that accounts for a weak coupling between cells. This parameter quantifies the weakening of the local dynamical rules due to the limited coupling of each individual cell to its local neighborhood. For different values of κ, different kinds of tumour are found, being able to reproduce tumours that resemble those in [8] and others that resemble those in [9], the type of tumours depending on the values of the parameter κ. In general, low values of κ tend to enforce the local rules over the ensemble while high values of κ are associated with limited intercellular communication [10]. Importantly, our model does not break any translation invariance. A tumour can start anywhere, not necessarily the center. Although the model is simple and deterministic, its output is unpredictable because it incorporates Conway's Game of Life as the cellular automaton governing the local dynamics in the limit $\kappa \to 0$. The deterministic character of the model, and the smoothing and loosening of the local dynamical rules, as the parameter κ is varied, are helpful to understand its intricate dynamics with the tools of bifurcation analysis and the qualitative theory of smooth nonlinear dynamical systems.

Parameter γ accounts for a global coupling. The local dynamics is coupled to the global average of the dynamical state of the cells in the lattice

$$u_t = \left\langle u_t^{i,j} \right\rangle := \frac{1}{\Omega} \sum_{i=1}^{n} \sum_{j=1}^{n} u_t^{i,j}. \tag{4}$$

We note that a tumour would grow without being stabilized if $\gamma = 0$. A non-vanishing global coupling is necessary for tumour volume stabilization. The way the latter enters in our model is analogous to the one found in models of spatiotemporal pattern formation in chemical systems [17]: the pressure has an stabilizing effect of the

homogeneous mode and creates a global coupling that is proportional to the lattice average of a local order parameter. This stabilizing effect is responsible, in our scenario, for the inhibition of the tumour growth.

2.1 Lattice and States

We consider square (Moore) neighborhoods of 3×3 sites. Using periodic boundary conditions in the lattice, the neighborhood of the site (i, j) is formed by the sites $(i + k, j + m)$ where k and m can take the values -1, 0 and 1. If a cancerous cell is in a stable state and is homogeneously surrounded in its neighborhood by stable cancerous cells with approximately the same value of their dynamical state, we say that the cell is necrotic.

The evolution of the state of site (i, j) at discrete time steps is given by

$$u_{t+1}^{i,j} = \mathcal{B}_\kappa\left(3 - s_t^{i,j},\ \frac{1}{2}\right) + u_t^{i,j}\mathcal{B}_\kappa\left(4 - s_t^{i,j},\ \frac{1}{2}\right) - \gamma u_t \tag{5}$$

where κ is the coupling parameter, γ is the global coupling strength parameter, and

$$s_t^{i,j} := \sum_{k,m=-1}^{1} u_t^{i+k,j+m} \tag{6}$$

is the neighborhood sum. The $\mathcal{B}_\kappa$ function [11] of real variables x and y is

$$\mathcal{B}_\kappa(x, y) := \frac{1}{2}\left[\tanh\left(\frac{x+y}{\kappa}\right) - \tanh\left(\frac{x-y}{\kappa}\right)\right] \tag{7}$$

For all finite values of x and y, the $\mathcal{B}_\kappa$ function satisfies the limits [11]:

$$\lim_{\kappa\to\infty} \mathcal{B}_\kappa\ (x,\ y) = 0 \qquad \lim_{\kappa\to\infty} \frac{\mathcal{B}_\kappa\ (x,\ y)}{\mathcal{B}_\kappa\ (0,\ y)} = 1 \tag{8}$$

$$\lim_{\kappa\to 0} \mathcal{B}_\kappa\ (x,\ y) = \mathcal{B}(x, y) = \frac{1}{2}\left(\frac{x+y}{|x+y|} - \frac{x-y}{|x-y|}\right) = \begin{cases} \operatorname{sgn} y & \text{if } |x| < |y| \\ \frac{\operatorname{sgn} y}{2} & \text{if } |x| = |y| \\ 0 & \text{if } |x| > |y| \end{cases} \tag{9}$$

where we have introduced the function $\mathcal{B}(x, y)$, which allows a universal map for cellular automata to be formulated [18].

In the limit $\kappa \to 0$ and in the absence of global coupling $\gamma = 0$, Eq. (5) becomes

$$u_{t+1}^{i,j} = \mathcal{B}\left(3 - s_t^{i,j}, \frac{1}{2}\right) + u_t^{i,j}\mathcal{B}\left(4 - s_t^{i,j}, \frac{1}{2}\right) = \begin{cases} 1 & \text{if } s_t^{i,j} = 3 \\ u_t^{i,j} & \text{if } s_t^{i,j} = 4 \\ 0 & \text{otherwise} \end{cases} \tag{10}$$

2.2 Relation to Conway's Game of Life

For Boolean initial conditions and $\kappa \to 0$ this model is similar to Conway's Game of Life [10, 18]:

1. *Any site in state* 1 *with fewer than two nearest neighbors in state* 1 *takes state* 0 *at the next time step.* The rule establishes the normalizing effect of the local neighborhood when normal cells predominate.
2. *Any site in state* 1 *with two or three nearest neighbors in state* 1 *remains in state* 1 *at the next time step.* The rule assumes that the normalization effect of the local neighborhood is lost when sufficient abnormal cells are present.
3. *Any site in state* 0 *with three nearest neighbors in state* 1 *changes to state* 1 *at the next time step.* The rule considers the promotion from a normal to an abnormal state.
4. *Any site in state* 1 *with more than three nearest neighbors in state* 1 *changes to state* 0 *at the next time step.* The rule establishes a limit to abnormal cell expansion, e.g. because of finite available resources, representing a change from positive to negative cooperativity.

Note that a predominantly normal neighborhood may constitute a normalizing microenvironment for a cell because of the abnormal cell underpopulation (rule 1). On the contrary, a significantly abnormal neighborhood may impair the normalization effect and promote the abnormal state (rules 2 and 3). In the case of abnormal cell overcrowding, however, limited proliferation could arise because of the competition for finite resources (rule 4) [10].

When $\kappa \neq 0$, Eq. (5) produces a more 'fuzzy' dynamics, and $u_t^{i,j}$ is a continuous variable. Further, we have:

5. *The coupling between sites due to the local rules 1 to 4 is modulated by the parameter* $\kappa \geq 0$. This parameter incorporates the collective influence of biological phenomena such as the stochastic intercellular diffusion of signaling molecules, the intrinsically probabilistic gene expression, and the individual cell heterogeneity. These noisy phenomena should weaken rules 1 to 4, which hold exactly only in the limit $\kappa \to 0$.
6. *A global coupling whose strength is given by a parameter* $\gamma \in [0, 1]$ *competes against the local inhomogeneities tending to stabilize a global homogeneous mode of normal cells*. The term $-\gamma u_t$ in Eq. (5) does not contribute significantly to the local dynamics if most cells in the lattice are normal, i.e., if $u_t \approx 0$. If many cells are abnormal, the term $-\gamma u_t < 0$ has a normalizing effect on an abnormal cell at position (i, j). The increased impact of the global coupling as the number of abnormal cells grow eventually stops the tumour growth. This global coupling represents the effect of the mechanical pressure.

When $\gamma > 0$ is increased, as shown in the next section, the homogeneous state consisting of normal cells tends to be more stable and the abnormal cells tend to be confined on a smaller region, where they tend to cluster and coalesce.

2.3 Mean-Field Approximation

Insight for the globally coupled case $\gamma \neq 0$ can be obtained using the analytical mean-field approximation in the absence of global coupling ($\gamma = 0$)

$$u_{t+1} = \mathcal{B}_\kappa\left(3 - 9u_t,\ \frac{1}{2}\right) + u_t \mathcal{B}_\kappa\left(4 - 9u_t,\ \frac{1}{2}\right) \tag{11}$$

where it is considered that all cells have approximately the same average value u_t, Eq. (4). The mean-field approximation provides a good description of the dynamics when κ is sufficiently large and is away of the cellular automaton limit. Let

$$f(u_t;\kappa) := \mathcal{B}_\kappa\left(3 - 9u_t,\ \frac{1}{2}\right) + u_t \mathcal{B}_\kappa\left(4 - 9u_t,\ \frac{1}{2}\right). \tag{12}$$

Then, a homogeneous fixed point u^* of Eq. (11) satisfies $u_{t+1} = u_t = u^*$, that is,

$$u^* = f(u^*;\kappa). \tag{13}$$

There is a homogeneous fixed point $u^*_{\text{norm}} \approx 0$ for every value of κ. In the cases $\kappa \to 0$ and $\kappa \to \infty$, we have, exactly, $u^*_{\text{norm}} = 0$. For finite non-vanishing κ values, the numerical solution of Eq. (13) shows that, in every case $u^*_{\text{norm}} < 0.15$. We call this the normalized homogeneous state, since all cells are normal, non-cancerous ones, at this fixed point.

Let $u_t = u^*_{\text{norm}} + \xi_t$, where ξ_t is a small perturbation around the fixed point. The evolution of the small perturbation is governed by the map

$$\xi_{t+1} = \left.\frac{\mathrm{d}f(x;\kappa)}{\mathrm{d}x}\right|_{x=u^*_{\text{norm}}} \xi_t \tag{14}$$

which is obtained by expanding Eq. (11) around u^*_{norm} in powers of ξ and retaining only the first term. Clearly, the perturbation from the normalized homogeneous state can only grow if

$$\left.\frac{\mathrm{d}f(x;\kappa)}{\mathrm{d}x}\right|_{x=u^*_{\text{norm}}} > 1. \tag{15}$$

The mean-field approximation with global coupling is

$$u_{t+1} = f(u_t;\kappa) - \gamma u_t, \tag{16}$$

an equation that has fixed points u^*_γ given by

$$u^*_\gamma = \frac{f(u^*_\gamma;\kappa)}{1+\gamma}. \tag{17}$$

As before, there is a normalized homogeneous fixed point $u^*_{\gamma,\mathrm{norm}}$ and linearization of Eq. (16) around it yields, for a small perturbation,

$$\xi_{t+1} = \left[\left. \frac{\mathrm{d}f(x;\kappa)}{\mathrm{d}x} \right|_{x=u^*_{\gamma,\mathrm{norm}}} - \gamma \right] \xi_t. \tag{18}$$

A perturbation can only grow if

$$\left. \frac{\mathrm{d}f(x;\kappa)}{\mathrm{d}x} \right|_{x=u^*_{\gamma,\mathrm{norm}}} > 1 + \gamma \tag{19}$$

where we see the stabilizing effect of the non-vanishing global coupling respect to the $\gamma = 0$ case: The larger the value of γ the less likely condition (19) is satisfied because $\mathrm{d}f(x;\kappa)/\mathrm{d}x|_{x=u^*_{\gamma,\mathrm{norm}}} \approx \mathrm{d}f(x;\kappa)/\mathrm{d}x|_{x=u^*_{\mathrm{norm}}}$.

2.4 Initial Conditions for Simulations

The lattice dynamics is studied using numerical simulations over a lattice with $159 \times 159 = 25281$ cells. We shall consider an initial condition consisting of a random distribution of 0 and 1 values in a 25×25 central square region ($N_{\mathrm{ab},0} = 123$ abnormal cells), the rest of the lattice being at state 0.

3 Results and Discussion

3.1 Spatiotemporal Dynamics in the Absence of Global Coupling ($\gamma = 0$)

To get insight in the full model with $\gamma \neq 0$, we first study the model in the absence of global coupling. For $\gamma = 0$ the model reduces to *Model II* discussed in our recent work [10].

Figure 1 shows the snapshots obtained for an inhomogeneous region occupying initially a central cluster. If $\kappa \gtrsim 1.9$ a homogeneous normal state is obtained at long times. As κ is decreased, the central inhomogeneity can grow unboundedly. Domain formation and oscillations are observed within the growing inhomogeneity. The number of abnormal cells N_{ab} grows until the whole lattice is occupied by abnormal cells.

The dynamics of the model can be analyzed further using the mean field approximation in the absence of global coupling, Eq. (11). We describe next the bifurcation diagram of Eq. (11) as κ is decreased from $\kappa \geq 2$ to 0:

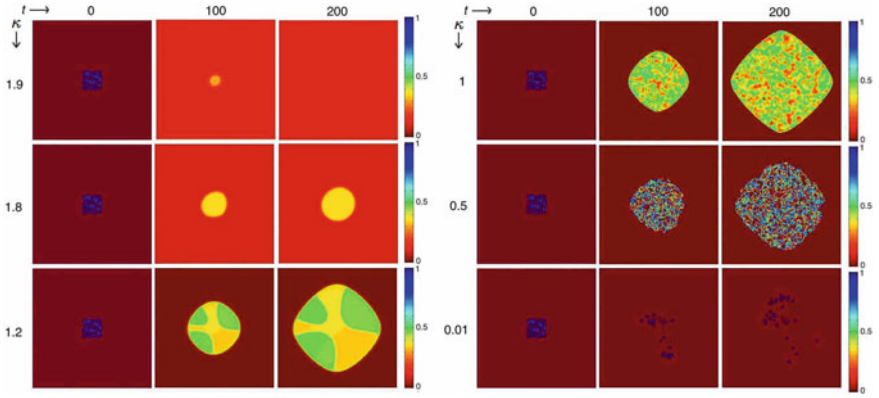

Fig. 1 Spatiotemporal evolution of the cell states $u_t^{i,j}$ obtained by iterating Eq. (5) in a multicellular ensemble of $159 \times 159 = 25281$ cells for six different κ values. The initial ($t = 0$) state is the same for all cases and consists of a random distribution of 0 and 1 values in a central square region of the lattice of 25×25 size, the rest of the lattice being at state 0 [10]

- A bifurcation is encountered at $\kappa \approx 1.95$, which is close to the value $\kappa \approx 1.9$ found in the numerical simulations of the exact dynamics, Eq. (5). The system abruptly splits into two branches leading to the bistable regime A (Fig. 2A). The two states correspond to a homogeneous abnormal (upper branch) and normal (lower branch) states. Remarkably, the system would tend to a normal homogeneous state when $\kappa \to 0$ only if the lower branch in Fig. 2A were followed, i.e., if the initial conditions were always constituted by a majority of normal cells, with a tiny and dilute proportion of abnormal cells.
- A bifurcation of the upper branch, representing the abnormal homogeneous state, is found at $\kappa \approx 1.35$ leading to two branches of abnormal states that perform period-2 oscillations. Further period doubling bifurcations between abnormal states are then observed at $\kappa \approx 1.2$ leading through a period-doubling cascade into chaos which is most prominent at $\kappa = 1$ (regime B in Fig. 2A). To substantiate this observation, we calculated the Lyapunov exponent λ showing that it is positive exactly in this regime [10] for initial conditions corresponding to an abnormal homogeneous state.
- In regimes C and D of Fig. 2A, the mean-field approximation, Eq. (11), fails because it can no longer be assumed that all neighborhoods are well described by an average cell value. Equation (5) needs to be considered in these regimes. Noise is high in regime C (see Fig. 1 for $\kappa = 0.5$) and more degrees of freedom are involved here in the spatiotemporal dynamics invalidating the mean field approximation.

The bifurcation diagram (Fig. 2) explains the pattern formation observed in Fig. 1 for $1 \leq \kappa \leq 1.9$: the upper branch with bifurcations corresponds to the abnormal region and the lower branch to the normal homogeneous region. The bifurcation

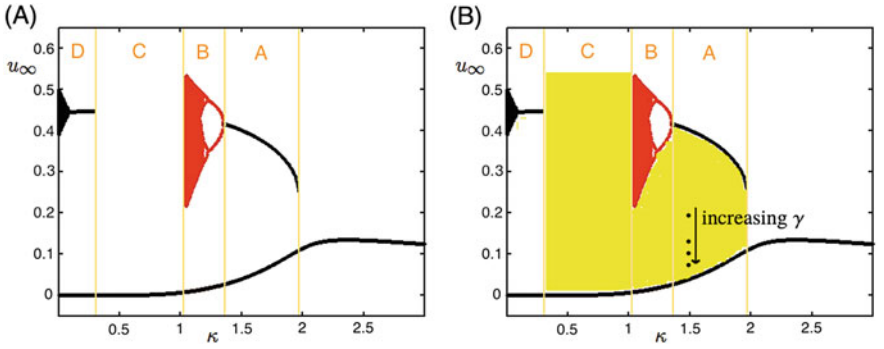

Fig. 2 Bifurcation diagram calculated from the asymptotic behavior of Eq. (11) in the absence **A** and in presence **B** of global coupling. The black curves correspond to stationary states u_∞ obtained at large times. The red points, following the branch of abnormal cell states, indicate the period doubling bifurcation cascades into chaos. The yellow region in **B** correspond to states that can be stabilized by means of a nonzero global coupling. These states (points marked) do not represent homogeneous states but the coexistence of normal and abnormal phases so that the global average value is u_∞. This phase coexistence corresponds to tumours of a fixed volume in the long time limit for initial conditions in which the abnormal cells are surrounded by a large homogeneous region of normal cells. Increasing γ leads to a larger fraction of normal cells in the coexisting phases

diagram also clarifies why oscillations occur only in the region of abnormal cells. Furthermore, as we see in the next section the bifurcation diagram allows to understand the spatiotemporal dynamics of the multicellular ensemble in the presence of a global coupling.

3.2 *Spatiotemporal Dynamics in the Presence of Global Coupling ($\gamma > 0$)*

As mentioned above, if there is initially a bounded region of abnormal cells in the lattice, the number of abnormal cells N_{ab} grows indefinitely until the whole lattice is filled with abnormal cells.

As we have explained in Sect. 2.2 the global coupling ($0 < \gamma \leq 1$) tends to stabilize a homogeneous state of normal cells. We now consider the introduction of a global coupling to the multicellular ensemble, aided by the insights provided by the bifurcation diagram in Fig. 2A. We note that the local spatiotemporal dynamics found in absence of global coupling is not significantly altered by the global coupling if: (1) the majority of the cells is in the normal state so that $u_t < 0.15$; (2) γ is small. The condition (1) is easily met if we consider initial conditions in which a tiny cluster of cells in the abnormal state is initially present. For the initial conditions employed in the simulations, we have that, at time $t = 0$, $\gamma u_0 = 123\gamma/25281 = 0.0049\gamma \leq 0.0049$, which makes the contribution of the global coupling to the spatiotemporal dynamics of the ensemble governed by Eq. (5) initially negligible.

Regions containing abnormal cells can coexist in a stable manner with regions containing only normal cells if a global coupling is added. When a global coupling is introduced, points in the yellow-shaded region of the bifurcation diagram in Fig. 2B can be stabilized in the long time limit. Points within the shaded region do not represent homogeneous states, but two-phase coexistence between regions of normal and abnormal cells. The simulations in Fig. 3 for increasing γ lie in regime A in Fig. 2B (four points shown). We have seen that in regime A there are two different stable branches, the normal and abnormal branches. Depending on the initial condition, in the absence of global coupling the trajectory is attracted to any of these branches. If we introduce a nonzero global coupling, both branches can coexist, and there are homogeneous regions in the lattice that can remain in the normal state and other connected regions in the abnormal state. If we start from a small cluster of abnormal cells surrounded by a homogeneous region of normal cells, we expect at initial times a behavior similar to the one found in Fig. 1 for $\kappa = 1.8$ and $\gamma = 0$. However, the growth of abnormal cells will stop if $\gamma \neq 0$: the contribution to the local dynamics due to the global coupling $-\gamma u_t$ grows and, for a sufficiently large contribution, normal cells at the boundary of the tumour are stabilized, precluding the growth of the latter.

In Fig. 3A the evolution of the number of abnormal cells $N_{\mathrm{ab}}(t)$ is shown for $\kappa = 1.5$ and the values of γ indicated on the curves. In Fig. 3B we show the results obtained by Gompertz's law

$$N_{\mathrm{ab}}(t) = N_{\mathrm{ab},0} \exp\left(\frac{A}{B}\left(1 - \exp(-Bt)\right)\right) \tag{20}$$

for $N_{\mathrm{ab},0} = 123$ and $A = 0.0211$, $B = 0.0047$ (curve a), $A = 0.0174$, $B = 0.0047$ (curve b), $A = 0.0140$, $B = 0.0044$ (curve c) and $A = 0.0096$, $B = 0.0035$ (curve d). Excellent agreement is obtained in all instances of the spatiotemporal evolution of the model and Gompertz's law.

The snapshots of the stable, stationary tumours obtained at time $t = 2000$ (Fig. 3C) show that the homogeneous region of normal cells grows and the region of cancerous cells shrinks when the global coupling strength increases. These tumours are like those described in Ref. [9]: the cells within the tumour are necrotic and only the cells at the perimeter of the tumour remain active. Regardless of the initial condition on a bounded region in the lattice, the tumour grows to a spherical shape. Even when the lattice is square and the underlying local dynamics is inherited from Conway's Game of Life, the smoothing parameter κ is responsible for a spatiotemporal evolution that is characteristic of a partial differential equation rather than that of a cellular automaton. As a consequence, isotropy is achieved.

The tumours reported in Ref. [8] behaved differently. Initially, the tumour quickly grows to a size that remains approximately constant while its perimeter fluctuates. The interior remains active for any long time even when the average number of abnormal cells saturates to a constant value, and those abnormal cells remain in a connected region of the same total area (disregarding small fluctuations). From the bifurcation diagram, Fig. 2A, we observed that, in regime C, in absence of global coupling noise

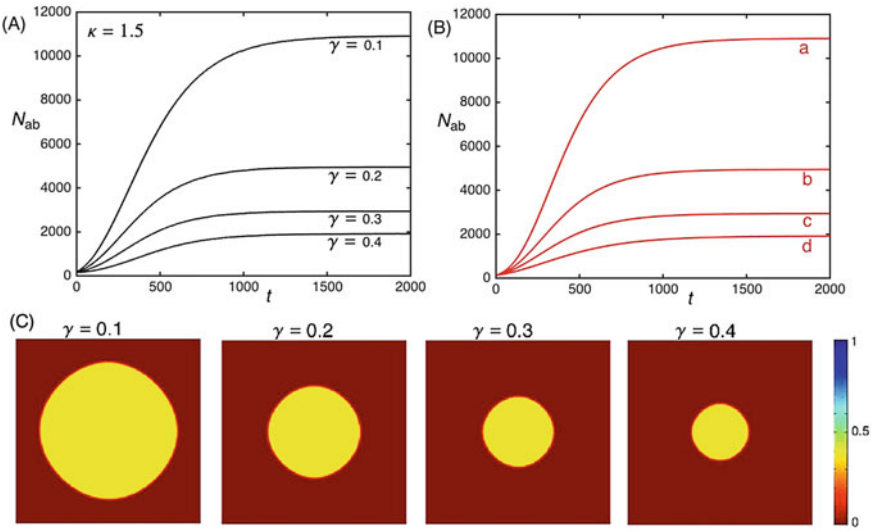

Fig. 3 Evolution of the number of abnormal cells $N_{ab}(t)$ on a lattice of $\Omega = 25281$ cells. **A** Results obtained from the model, Eq. (5), for $\kappa = 1.5$ and the values of γ indicated below the curves, by using Eq. (3) to count the abnormal cells. **B** Results obtained by the Gompertz law, Eq. (20) for $N_{ab,0} = 123$ and $A = 0.0211$, $B = 0.0047$ (curve a), $A = 0.0174$, $B = 0.0047$ (curve b), $A = 0.0140$, $B = 0.0044$ (curve c) and $A = 0.0096$, $B = 0.0035$ (curve d). **C** Snapshots at time $t = 2000$ of the stable, stationary tumours. This tumour behavior is similar to that reported in Ref. [9].

is high in the branch of abnormal cells and the mean field approximation breaks down: more degrees of freedom are needed to describe the branch of abnormal cells that becomes essentially inhomogeneous. In Fig. 1 it is observed that for $0.3 \leq \kappa \leq 1$ a cluster of active abnormal cells grows from an initial condition where only a few cells are abnormal. The cluster of active abnormal cells against the homogeneous region of normal cells grows until the whole lattice is filled in absence of global coupling. For $\gamma > 0$ it is now possible to stabilize a significant part of the normal region, leading to saturation of the tumour growth. Therefore, tumours like those reported in Ref. [8] can be predicted by our model for κ parameter values in the range $0.3 \leq \kappa \leq 1$ and $\gamma > 0$. In Fig. 4 we show that $\kappa = 0.9$ and $\gamma = 0.9$ describe a tumour growth behavior similar to that of Ref. [8].

In Fig. 5, the evolution of the number of abnormal cells $N_{ab}(t)$ is shown for $\kappa = 0.9$ and the values of γ indicated on the curves. The black curves are the results obtained from the model, Eq. (5). The red curves represent Gompertz's law, Eq. (20) for $N_{ab,0} = 123$ and $A = 0.0458$, $B = 0.0105$ (curve a), $A = 0.0481$, $B = 0.0120$ (curve b) and $A = 0.0524$, $B = 0.0150$ (curve c). Excellent agreement is obtained in both instances of the averaged spatiotemporal evolution of the model and Gompertz's law. The snapshots of the stable, stationary tumours obtained at time $t = 2000$ (Fig. 5B) show that the homogeneous region of normal cells grows and the region of

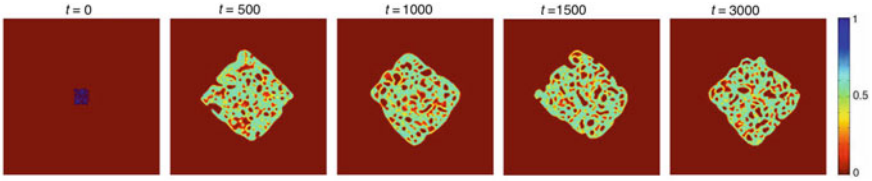

Fig. 4 Snapshots of the spatiotemporal evolution of the cell states obtained for $\kappa = 0.9$ and $\gamma = 0.9$ at the times indicated on the panels. The initial state is also shown. This tumour behavior is similar to that reported in Ref. [8]

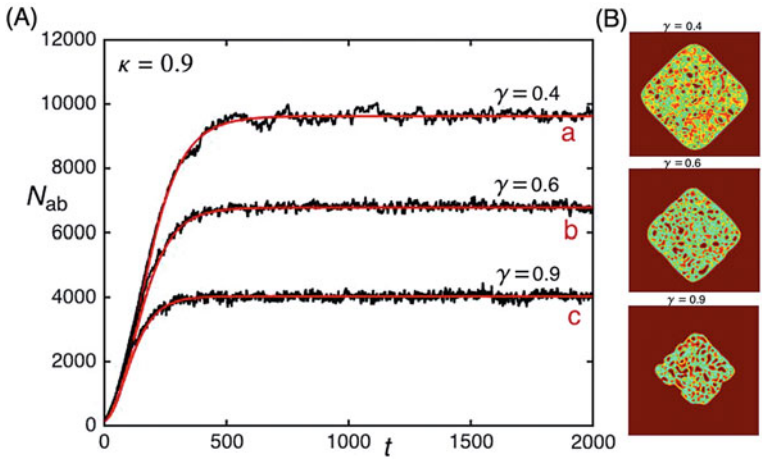

Fig. 5 Evolution of the number of abnormal cells $N_{\mathrm{ab}}(t)$ on a lattice of $\Omega = 25281$ cells. **A** Results obtained from the model, Eq. (5), for $\kappa = 0.9$ and the values of γ indicated on the curves (black curves). The red curves are the representations of Gompertz's law, Eq. (20), for $N_{\mathrm{ab},0} = 123$ and $A = 0.0458$, $B = 0.0105$ (curve a), $A = 0.0481$, $B = 0.0120$ (curve b) and $A = 0.0524$, $B = 0.0150$ (curve c). **B** Snapshots of the tumours at time $t = 2000$. Although their interior is not stationary but dynamical, the area occupied by the tumour is constant and remains connected

cancerous cells shrinks when the global coupling strength increases. These tumours are like those described in Ref. [8]: not only the cells in the perimeter of the tumour are active, but also those in the interior. The tumour grows up to a maximal size and remains bounded, although the fluctuations of both the interior of the tumour and its perimeter persist. This is the case, regardless of the initial condition on a bounded region in the lattice.

For $\kappa = 0.9$ and increasing global coupling, $\gamma = 0.4$, 0.5, 0.6, 0.7, 0.8 and 0.9, the parameters A and B calculated by fitting Gompertzian curves, Eq. (20) are obtained. A linear correlation with coefficient of determination $R^2 = 0.995$ is obtained between $\exp A$ and $\ln B$, such that $\exp A \approx 0.020 \ln B + 1.138$. We thus observe that the parameters calculated for the Gompertzian curves that fit the results from our model satisfy the linear correlation reported by Norton et al. [5] for experimental biological instances of tumour growth (Fig. 6).

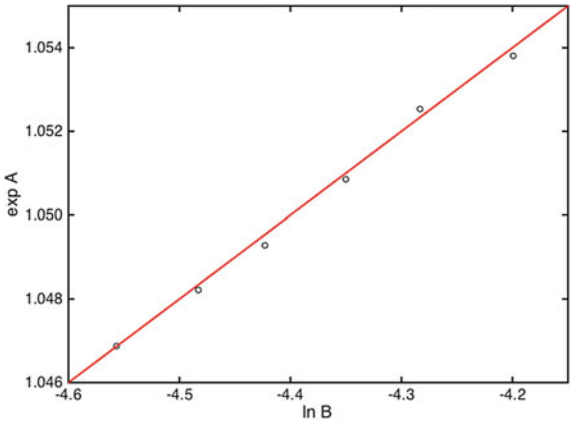

Fig. 6 The parameters A and B of the Gompertzian curves fitting the spatiotemporal evolution of the tumour dynamics predicted by the model, Eqs. (3) and (5) for $\kappa = 0.9$ and $\gamma = 0.4$, 0.5, 0.6, 0.7, 0.8 and 0.9 show an excellent agreement with the empirical relation found in Ref. [5], Eq. (2). From these simulation results, the parameter values in Eq. (2) are determined as $a = 0.020 \pm 0.002$ and $b = 1.138 \pm 0.008$

Parameters a and b in Eq. (2) depend on the type of cancer under consideration. In our model, these parameters exclusively depend on κ, a parameter which, as we have seen, yields different types of tumours depending on the regime found in the bifurcation diagram in Fig. 2.

Values of κ in the interval $1.35 \leq \kappa \leq 1.95$ (regime A in Fig. 2), yields tumours composed of necrotic, inactive cancerous cells like those found in Ref. [9]. Values of κ in the range $1 \leq \kappa \leq 1.35$ (regime B in Fig. 2) yield tumours bounded by a circular shape as those in the interval $1.35 \leq \kappa \leq 1.95$ but their interior is now active, presenting coherent periodic oscillations in different domains of the tumour ($1.18 \leq \kappa \leq 1.35$) or chaotic, aperiodic behavior ($1 \leq \kappa \leq 1.15$). Values of κ in the interval $0.3 \leq \kappa \leq 1$ (regime C in Fig. 2) yields tumours composed of active cancerous cells like those found in Ref. [8]. The difference between these tumours and those found in Regime B is that the perimeter of the tumour is not a circumference but a complex, dynamically-changing, shape. Finally, values of κ in the range $0 \leq \kappa \leq 0.3$ (regime D in Fig. 2) correspond to the cellular automaton limit of the map and do not yield connected tumours.

4 Conclusions

A coupled map lattice that simulates Gompertz tumour growth as an emergent behavior has been presented. The model, Eq. (5), depends only on two free parameters, κ and γ, that control the strengths of the intercellular and global couplings, respectively. The model displays the correlations between parameters in the Gompertz

tumour growth model [5], an important feature used in cancer diagnosis to predict long-time behavior from early stages of tumour development. Previous cellular automata models [8, 9, 19] have not addressed these correlations and depend on a larger number of parameters.

As the intercellular coupling parameter κ is varied, different types of tumours are modelled. On one hand, for κ large, the model describes tumours that are only active at the surface, the interior of the tumour being mostly composed of necrotic, inactive cells [9]. These tumours, with homogeneous interior, are well described by the mean-field approximation of the model, Eq. (11). As κ is lowered from $\kappa = 1.35$, the degree of inner activity of the tumour can be switched from coherent and periodic to aperiodic and chaotic. As κ is further lowered below $\kappa = 1$, more degrees of freedom become active, the mean-field approximation, Eq. (11), breaks down, and the model reproduces tumours that are active and noisy not only at its surface but also in its interior [8]. On the contrary, previous models accounted only for one type of tumour.

Growth inhibition and tumour volume saturation is described by a global coupling that can represent the contribution of the mechanical pressure, limited amount of nutrients, chemical inhibitors, etc. Importantly, the tumour growth is not here artificially constrained as in previous models in which the dynamics of the tumour was made explicitly dependent on the radius or the volume of the tumour in an ad hoc manner. Geometric features of the tumour do not enter in the model as explicit variables but arise as an emergent phenomenon as a consequence of the spatiotemporal dynamics. This feature is important because, in contrast with previous approaches, the tumour does not need to start 'at the center of the lattice' but can start from any other place. The model is translationally invariant: the local dynamics is the same in every site of the lattice.

Compared to previous cellular automata models applied to tumour growth that are all probabilistic, our model is deterministic and it is given by a simple map, Eq. (5), that can be iterated on a lattice. However, in spite of being deterministic, our coupled map lattice incorporates Conway's Game of Life as a cellular automaton limit ($\kappa \to 0$) and, therefore, yields complex unpredictable behavior for arbitrary initial conditions. Quite remarkably, for $\kappa > 1$ the model yields isotropic growth in spite of taking place on a square lattice.

Gompertzian growth behavior has been found for all different kinds of tumour, independently of the value of the parameter κ. Thus, our model suggests that Gompertzian growth has a universal character, as pointed out by previous macroscopic approaches [5, 7].

References

1. Kraus, M., Wolf, B.: Emergence of self-organization in tumor cells: relevance for diagnosis and therapy. Tumor Biol. **14**, 338–353 (1993). https://doi.org/10.1159/000217849

2. Brunton, G.F., Wheldon, T.E.: Prediction of the complete growth pattern of human multiple myeloma from restricted initial measurements. Cell Tissue Kinet. **10**, 591–594 (1977). https://doi.org/10.1111/j.1365-2184.1977.tb00316.x
3. Steel, G.G.: Growth Kinetics of Tumours. Clarendon Press, Oxford (1977)
4. Klein, C.A.: Parallel progression of primary tumours and metastases. Nat. Rev. Cancer **9**, 302–312 (2009). https://doi.org/10.1038/nrc2627
5. Norton, L., Simon, R., Brereton, H.D., Bogden, A.E.: Predicting the course of Gompertzian growth. Nature **264**, 542–545 (1976). https://doi.org/10.1038/264542a0
6. Norton, L.: A Gompertzian model of human breast cancer growth. Cancer Res. **48**, 7067–7071 (1988)
7. Benzekry, S., Lamont, C., Beheshti, A., Tracz, A., Ebos, J.M.L., et al.: Classical mathematical models for description and prediction of experimental tumor growth. PLoS Comput. Biol. **10**(8), e1003800 (2014). https://doi.org/10.1371/journal.pcbi.1003800
8. Qi, A.-S., Zheng, X., Du, C.-Y., An, B.-S.: A cellular automaton model of cancerous growth. J. Theor. Biol. **161**, 1–12 (1993). https://doi.org/10.1006/jtbi.1993.1035
9. Kansal, A.R., Torquato, S., Harsh, G.R., IV., Chiocca, E.A., Deisboeck, T.S.: Simulated brain tumor growth dynamics using a three-dimensional cellular automaton. J. Theor. Biol. **203**, 367–382 (2000). https://doi.org/10.1006/jtbi.2000.2000
10. García-Morales, V., Manzanares, J.A., Mafé, S.: Weakly coupled map lattice models for multicellular patterning and collective normalization of abnormal single-cell states. Phys. Rev. E **95**, 042324 (2017). https://doi.org/10.1103/physreve.95.042324
11. Garcia-Morales, V.: From deterministic cellular automata to coupled map lattices. J. Phys. A.: Math. Theor. **49**, 295101 (2016). https://doi.org/10.1088/1751-8113/49/29/295101
12. Berlekamp, E.R., Conway, J.H., Guy, R.K.: Wining Ways for Your Mathematical Plays, vol. 2. Academic Press, New York (1982)
13. Adamatzky, A. (ed.): Game of Life Cellular Automata. Springer, New York (2010)
14. Adachi, S., Peper, F., Lee, J.: The Game of Life at finite temperature. Phys. D **198**, 182 (2004). https://doi.org/10.1016/j.physd.2004.04.010
15. Chua, L.O., Roska, T., Venetianer, P.L.: The CNN is universal as the Turing machine. IEEE Trans. Circuits Syst. I **40**, 289 (1993). https://doi.org/10.1109/81.224308
16. Pazienza, G.E., Gomez-Ramirez, E., Vilasi's-Cardona, X.: Polynomial cellular neural networks for implementing the Game of Life. In: Marques de Sá, J., Alexandre, L.A., Duch, W., Mandic, D.P. (eds.) Proceedings of ICANN 2007. LNCS, vol. 4668, pp. 914–923. Springer, Berlin (2007). https://doi.org/10.1007/978-3-540-74690-4-9
17. Mertens, F., Imbihl, R., Mikhailov, A.: Breakdown of global coupling in oscillatory chemical reactions. J. Chem. Phys. **99**, 8668 (1993). https://doi.org/10.1063/1.465590
18. García-Morales, V.: Universal map for cellular automata. Phys. Lett. A **376**, 2645 (2012). https://doi.org/10.1016/j.physleta.2012.07.021
19. Deutsch, A., Dormann, S.: Cellular Automaton Modeling of Biological Pattern Formation: Characterization, Applications and Analysis. Birkhäuser, Boston (2005)